STOCHASTIC GROUND MOTION SIMULATION WITH GEOLOGICAL SITE EFFECTS IN DAMAGE ASSESSMENT

João M. C. Estêvão

Escola Superior de Tecnologia, Universidade do Algarve, Faro, Portugal

Carlos Sousa Oliveira

Instituto Superior Técnico, Departamento de Engenharia Civil e Arquitectura, Lisbon, Portugal

SUMMARY

Damage assessment of structures with a mechanical non linear model demands the representation of seismic action in terms of an accelerogram (dynamic analysis) or a response spectrum (pushover analysis). Stochastic ground motion simulation is largely used in regions where seismic strong-motion records are available in insufficient number. In this work we present a variation of the stochastic finite-fault method with dynamic corner frequency that includes the geological site effects. The method was implemented in a computer program named SIMULSIS that generate time series (accelerograms) and response spectra. The program was tested with the M_W= 7.3 Landers earthquake (June 28, 1992) and managed to reproduce its effects. In the present work we used it to reproduce the effects of the 1980's Azores earthquake (January 1, 1980) in several islands, with different possible local site conditions. In those places, the response spectra are presented and compared with the buildings damage observed.

1. INTRODUCTION

In the Eurocode 8 (CEN, 2004), the time-history representation of seismic action is classified in three groups: artificial accelerograms (synthetic accelerograms generated so as to mach an elastic response spectra), recorded accelerograms and simulated accelerograms (synthetic accelerograms generated through a physical simulation of source and travel path mechanisms).

The use of artificial accelerograms, for a structural engineer, is very attractive, mainly because doesn't depend on seismological knowledge. Is now widely accepted that the use of artificial accelerograms, in seismic non-linear analysis, have many problems. Such as the fact that these accelerograms tend to be particularly unrealistic (Bommer and Acevedo, 2004).

For regions with medium to low seismicity, and with lack of strong-motion records, the use of recorded accelerograms is a problematic issue. In these areas, the use of simulated accelerograms can be a valid alternative. Portugal is an example of such a problem, where the historical knowledge of massive destruction due the 1755 earthquake exists, but not enough strong-motion records for engineering purposes are available.

There are plenty of methods for generation of simulated accelerograms (Erdic and Durukal, 2006; Stewart *et al.*, 2001) which can be divided in three major groups: deterministic methods, stochastic methods and hybrid methods.

In the deterministic methods, seismic wave propagation in heterogeneous media is expressed by the numerical solution of the equations of 3D motion and the constitutive relationship between stress and strain of the wavefield, so that the seismic action is represented in terms of velocity and involves enormous computing time consuming work (Furumura, 2005).

In practical problems of structural engineering, non linear analysis demands the use of simulated accelerograms with spectral energy content between 0.5 and 30 Hz (Lee, 1995). Deterministic methods are almost impossible to use for structural analysis with current computers, because they require very dense grid points to fulfil the demand of energy frequency content.

The deterministic methods are the only ones that can reproduce, in a realistic manner, the influence of path effects, including small-scale heterogeneities in the subsurface structure, so they are very important in seismological studies. Synthetic waveforms have been generated for Portugal with deterministic models, to study several past earthquakes (Borges *et al.*, 2007a; Borges *et al.*, 2007b).

Many stochastic methods have been proposed based on Boore approach (Boore, 1983; 2003), in which a white-noise time series is adjusted to a seismological determined point-source Fourier spectrum.

These methods are less time consuming and can simulate accelerograms with the desired frequency content. The program LNECLOSS (Campos Costa *et al.*, 2004; Campos Costa *et al.*, 2006) is an example of a computer implementation of stochastic methods, only in frequency domain, used for Portugal seismic risk assessment.

The hybrid methods results from a combination of the two approaches described earlier.

This work presents a stochastic method which considers the existence of asperities in fault plane, and non-linear geological site effects in the simulation of ground motion. The method was implemented in a computer program named SIMULSIS, developed in Object Pascal for Windows, with DELPHI2007 (CodeGear, 2007).

2. PROGRAM SIMULSIS

2.1. Finite fault model

The methodology implemented in SIMULSIS was based in several concepts that support the program EXSIM (Motazedian and Atkinson, 2005). The simulated accelerogram results from the contribution of a number of small earthquakes as subfaults that comprise a big fault (Figure 1).

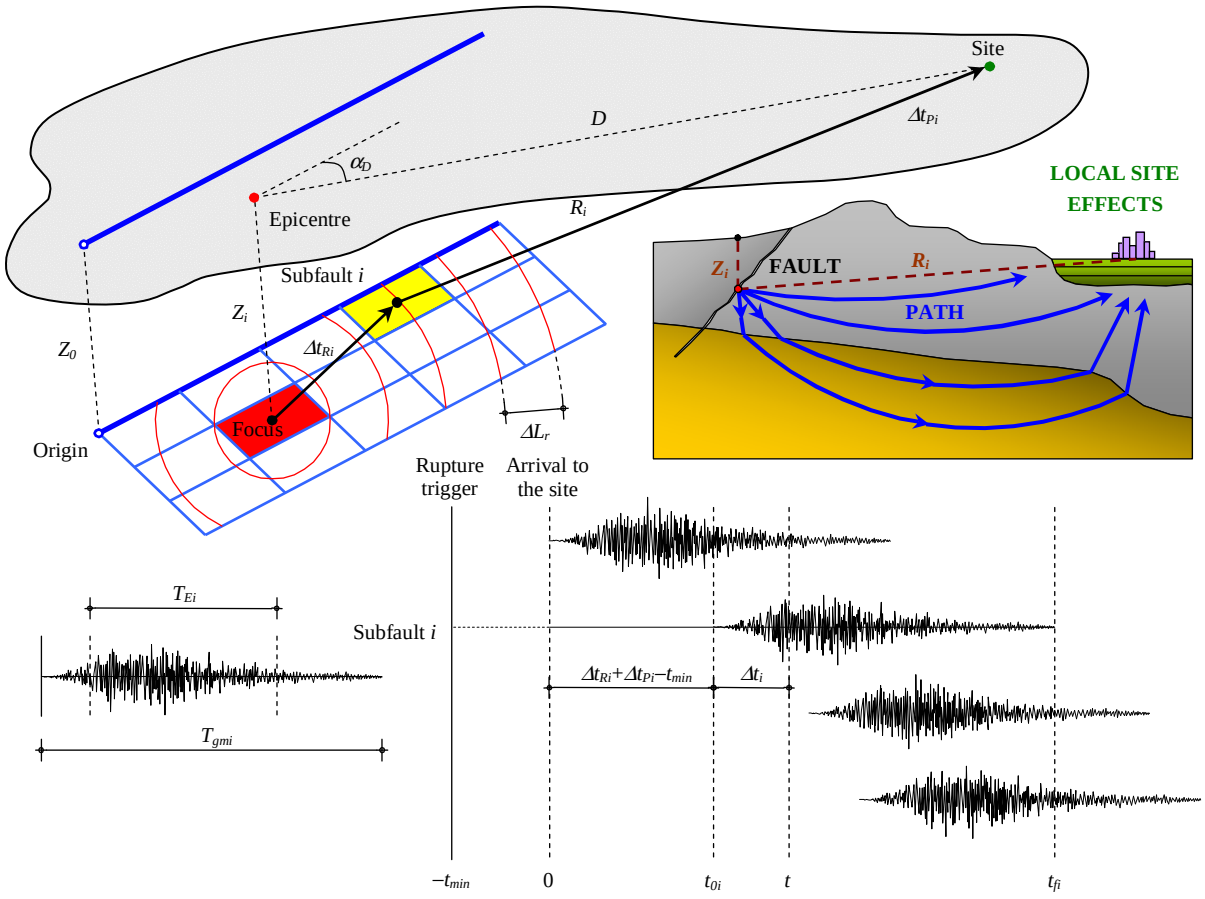

Figure 1 – Scheme of the methodology implemented in SIMULSIS

A large fault is divided in N_F subfaults and each subfault is considered as a point-source event. In SIMULSIS the rupture spreads radialy from the hypocenter, with a constant velocity V_r, so time series results from a superposition of sinusoidal waves, with circular frequencies ω_n and random phase angles θ_{ni} (distributed uniformly between 0 to 2π rad), that are summed with a proper delay

$$a_{g\,(t)} = \sum_{i=1}^{N_F} \sum_{n=1}^{N_{\omega i}} A_{i,n\,(\Delta t_i)} \cdot \cos\left(\omega_n \cdot \Delta t_i + \theta_{n,i}\right) \tag{1}$$

$$\Delta t_i = t - t_{0i} = t - \left(\Delta t_{Ri} + \Delta t_{Pi} - t_{\min}\right) \quad , \quad 0 \le \Delta t_i \le T_{gmi} \tag{2}$$

The wave amplitude $A_{i,n(\Delta ti)}$ is the contribution of the point-source i to the frequency n.

The spectrum of the ground motion of each subfault is an essential part of the stochastic method. It is convenient to break the total spectrum $A_i(\omega,M_{0i},R_i)$ of the motion at a site into contributions from subfault source $F_i(\omega,M_{0i})$, path $P_i(\omega,R_i)$ and local site effects $L(\omega)$, as it is represented in Figure 1 (Boore, 1983; 2003).

$$A_i\left(\omega, M_{0i}, R_i\right) = F_i\left(\omega, M_{0i}\right) \cdot P\left(\omega, R_i\right) \cdot L\left(\omega\right) \tag{3}$$

2.2. Subfault point-source

For each subfault, the source spectrum of shear waves can be modelled by

$$F_i\left(\omega, M_{0i}\right) = H_i \cdot H_{(\omega)} \cdot C_{0i} \cdot M_{0i} \cdot A_{0i}\left(\omega\right) \tag{4}$$

where H_i and $H_{(\omega)}$ are scaling factors which conserves the total radiated energy at the source, M_{0i} is the seismic moment (dyne-cm) of the subfault i, and C_{0i} is a constant given below

$$C_{0i} = \frac{R_{\theta\phi i} \cdot C_V \cdot C_F}{4\pi \cdot \rho \cdot \beta^2 \cdot R_0} \times 10^{-20} \tag{5}$$

in which $R_{\theta\phi i}$ is the radiation pattern of the subfault i, C_V represents the partition of total shear-wave energy into horizontal components $\left(=1/\sqrt{2}\right)$, C_F is the effect of the free surface (equal to 2 for SH waves), ρ (gm/c^3) and β (km/s) are the density and shear-wave velocity in the vicinity of the source, R_0 (= 1 km) is a reference distance, and $A_{0i}(\omega)$ is an acceleration spectrum (Boore, 1983; 2003).

$$A_{0i}\left(\omega\right) = \frac{\omega^2}{1 + \left(\dfrac{\omega}{\omega_{ci}}\right)^2} \tag{6}$$

The dynamic corner frequency of the subfault i is related to static stress drop ($\Delta\sigma$ in bars), and is given by:

$$\omega_{ci} = 2 \cdot \pi \cdot 4.9 \times 10^6 \cdot \beta \cdot \left(\frac{\Delta\sigma}{N_R\left(\Delta t_{Ri}\right) \cdot M_0}\right)^{\frac{1}{3}} \tag{7}$$

It was adopted the concept of active pushing area ΔL_r (Motazedian and Moinfar, 2006), but with $N_R(\Delta t_{Ri})$ representing the cumulative percentage of ruptured subfaults, in terms of seismic moment, between the most distant (less or equal to ΔL_r) subfault N_0 and the subfault i, given by

$$N_R(\Delta t_{Ri}) = \frac{1}{M_0} \cdot \sum_{n=N_0}^{i} M_{0n} \tag{8}$$

To account the existence of asperities, the seismic moment of each subfault i is related to the displacement pattern (Δu_i) at the fault, by:

$$M_{0i} = \frac{\Delta u_i}{\sum_{j=1}^{N_F} \Delta u_j} \cdot M_0 \tag{9}$$

The scaling factor H_i guaranties the subfault energy conservation at high frequencies. The SIMULSIS have the option of using two different expressions for the determination of H_i, which are:

$$H_i = \sqrt{\frac{M_0}{M_{0i}} \cdot \frac{\sum_{\omega} [A_0(\omega)]^2}{\sum_{\omega} [A_{0i}(\omega)]^2}} \tag{10}$$

similar to the expression that is implemented in EXSIM program, or

$$H_i = \sqrt{\frac{1}{N_F} \cdot \frac{[A_0(\infty)]^2}{[A_{0i}(\infty)]^2}} \tag{11}$$

The scaling factor $H_{(\omega)}$ corrects the total energy content at all frequencies, and is given by:

$$H_{(\omega)} = \frac{\int_0^{\omega} [M_0 \cdot A_0(\omega)]^2 \, d\omega}{\sum_{i=1}^{N_F} \int_0^{\omega} [H_i \cdot M_{0i} \cdot A_{0i}(\omega)]^2 \, d\omega} \tag{12}$$

The SIMULSIS have the option of using a constant value for the radiation pattern, which is 0.55 (Boore and Boatwright, 1984), or a different value for each subfault (Figure 2).

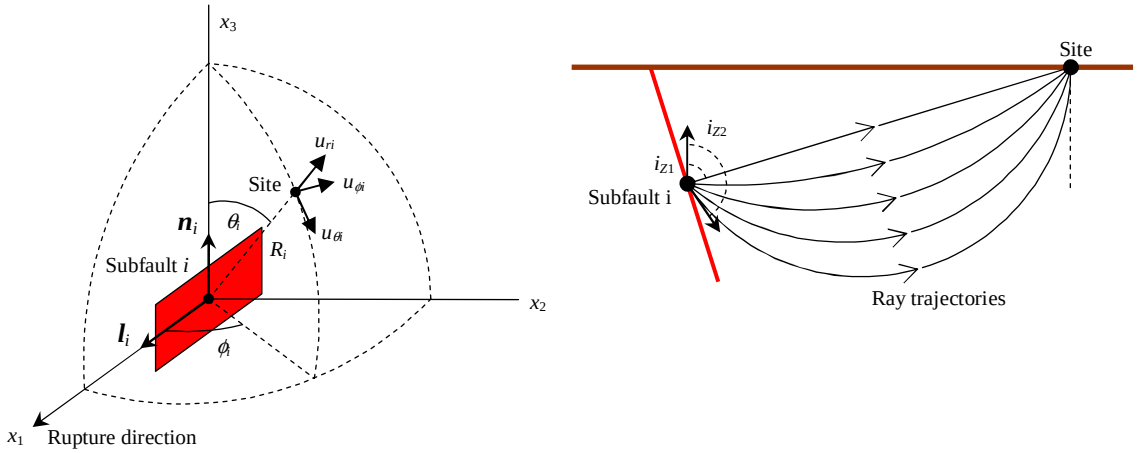

Figure 2 – Scheme for determination of radiation pattern

For each subfault, the two components of S waves, have normalized amplitudes given by (Udías, 1999):

$$\text{S1:} \quad u_{\theta i} = \cos(2\theta_i) \cdot \cos(\phi_i) \tag{13}$$

$$\text{S2}: \quad u_{\varphi i} = \cos(\theta_i) \cdot \sin(\varphi_i) \tag{14}$$

SIMULSIS calculate the radiation pattern by considering the mean value between two ray trajectories, a direct path (i_{z1}) and an indirect path (i_{z2}) that is tangent to the vertical direction at the site.

The mean value of the theoretical radiation pattern is given by

$$R_{\theta\phi i} = \frac{1}{i_{Z2} - i_{Z1}} \cdot \int_{i_{Z1}}^{i_{Z2}} \left| l_i \cdot u_{\theta i} + n_i \cdot u_{\phi i} \right| \cdot di_Z \tag{15}$$

which is then adjust to account the difference between the mean theoretical value of 0.63 and the observed value of 0.55 proposed by Boore and Boatwright (1984).

2.3. Path effects

The path effects are represented by combination of two functions, given by

$$P(\omega, R_i) = P_A(\omega, R_i) \cdot P_G(R_i) = \exp\left[-\frac{\omega \cdot R_i}{2 \cdot Q(\omega) \cdot c_Q} \right] \cdot \begin{cases} \dfrac{R_0}{R_i}, & R_i \le R_1 \\ P_G(R_1) \cdot \left(\dfrac{R_1}{R_i} \right)^{p1}, & R_1 < R_i \le R_2 \\ \vdots & \\ P_G(R_n) \cdot \left(\dfrac{R_1}{R_i} \right)^{pn}, & R_n \le R_i \end{cases} \tag{16}$$

where $P_G(R_i)$ accounts for geometrical spreading of seismic energy and $P_A(\omega,R_i)$ for anelastic attenuation.

The geometrical spreading function is given by a piecewise continuous series of straight lines, and the anelastic attenuation is a function of quality factor $Q(\omega)$, in which c_Q is the velocity of seismic waves used in the determination of $Q(\omega)$.

2.4. Local site effects

In the program SIMULSIS, local site effects are divided in two functions:

$$L(\omega) = H_R(\omega) \cdot H_S(\omega) \tag{17}$$

$H_R(\omega)$ is a filter that accounts for the diminution of the high-frequency motions in a rock outcropping reference site, and can be given by the combination of two filters (Boore, 2003):

$$H_R(\omega) = \left[1 + \left(\frac{\omega}{\omega_{\max}} \right)^8 \right]^{-\frac{1}{2}} \cdot \exp\left(-\frac{k_0 \cdot \omega}{2} \right) \tag{18}$$

where ω_{max} ($=2\pi \cdot f_{max}$) is the cut-off frequency and k_0 is a diminution parameter.

SHAKE91 (Idriss and Sun, 1992), a version of SHAKE (Schnabel *et al.*, 1972), is a commonly used and referenced computer program for geotechnical earthquake engineering. In this kind of programs, the non-linear soil transfer function for S waves is obtained from an equivalent linear analysis of a one-dimensional "soil column". This procedure was implemented in the program SIMULSIS, in which

$$H_S(\omega) = \frac{|u_1|}{|u_{NN}|} = \frac{A_1}{A_{NN}} \tag{19}$$

$$u_m = u_m(z,t) = \left(A_m \cdot e^{i \cdot \lambda_m^* \cdot z} + B_m \cdot e^{-i \cdot \lambda_m^* \cdot z} \right) \cdot e^{i \cdot \omega t} \tag{20}$$

with complex wave number given by

$$\lambda_m^* = \sqrt{\frac{\rho_m \cdot \omega^2}{G_m \cdot (1 + 2 \cdot i \cdot \xi_m)}} \tag{21}$$

where ρ is the unit mass, G is the shear modulus and ξ is the damping ratio of the soil layer m.

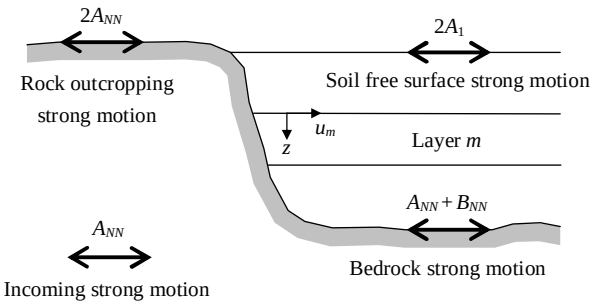

Figure 3 – Site response analysis

2.5. Time series

The strong motion duration (T_E) may be represented as the sum of the duration of rupture process (T_F), the duration due to propagation path effects (T_P) and the prolongation of the motion caused by local site conditions (T_L) (Lee, 2002):

$$T_E = T_F + T_P + T_L \tag{22}$$

The total duration of the ground motion can be defined as

$$T_{gm} = N_\eta \cdot T_E \tag{23}$$

The definition of earthquake duration is very important in time-domain simulations for structures non-linear analysis. In this paper we adopt the concept of effective duration which is the interval of time between two limits of the accelerogram Arias intensity (Bommer and Martinez-Pereira, 1999).

A simulated point-source accelerogram for subfault *i*, with non-stationary frequency content, can be represented by

$$a_{g(t)} = \sum_{n=1}^{N_\omega} \sqrt{2 \cdot G_{ai}(t,\omega_n) \cdot \Delta\omega} \cdot \cos(\omega_n t + \theta_n) \tag{24}$$

where the non-stationary power spectral density function is

$$G_{ai}(\omega,t) = g_i(t)^2 \cdot G_{ai}(\omega) \tag{25}$$

in which $g_i(t)$ is a deterministic envelope function and $G_{ai}(\omega)$ is a stationary power spectral density function (Gupta and Trifunac, 1996).

In program SIMULSIS was implemented the envelope presented in Figure 4, which is an adjustment to the envelope function implemented in point-source program SMSIM (Boore, 2005).

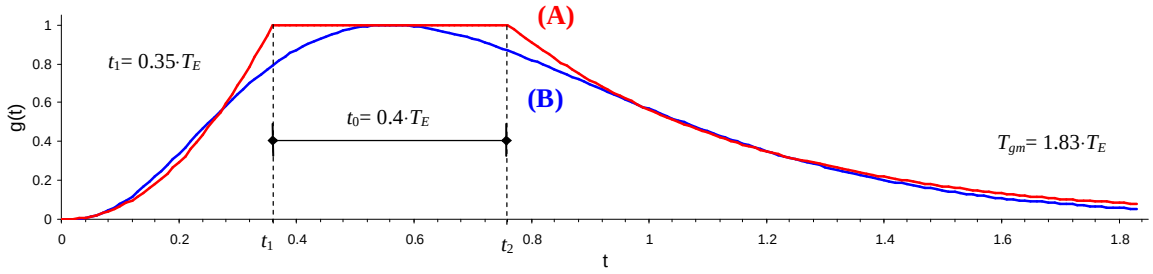

Figure 4 – Envelope function adopted in (A) SIMULSIS compared with implemented in (B) SMSIM

For each point-source, the stationary power spectral density function can be related to the Fourier amplitude spectrum (Kramer, 1996), and is given by

$$G_{ai}(\omega) = \frac{F_i(\omega, M_{0i})^2}{\pi \cdot T_F} \tag{26}$$

so

$$A_{i,n(t)} = g_i(t) \cdot \sqrt{\frac{2 \cdot \Delta\omega_i}{\pi \cdot T_F}} \cdot F_i(\omega_n, M_{0i}) \cdot P(\omega_n, R_i) \cdot L(\omega_n) \tag{27}$$

3. PROGRAM VALIDATION

For the validation of the computer program SIMULSIS, we compared the response spectra of the simulated accelerograms with the response spectra of the records obtained after the 28 June 1992 Landers earthquake, in California.

Several time-domain simulations were made for three sites around the rupture (Figure 5):

• Silent Valley/Poppet Flat (CGS - CSMIP Station No. 12206), 33.851N 116.852W, 1098 m of altitude, weathered granite, 56.015 km to epicentre (α_D = 66.180º).

• Lake Cahuilla/County Park (CGS - CSMIP Station No. 12624), 33.628N 116.28W, 35 m of altitude, hard granodiorite bedrock, 66.793 km to epicentre (α_D = 10.139º).

• Pearblossom/Pallet Creek (CGS - CSMIP Station No. 23584), 34.458N 117.909W, 1206 m of altitude, granitic rock, 138.348 km to epicentre (α_D= 141.250º).

The Landers earthquake resulted from lateral shear of five major faults, with different directions, within an 80 km wide belt. Its seismic moment of 10^{27} dyne-cm is equivalent to a magnitude M_w of 7.3 (Sieh *et al.*, 1993).

Because of SIMULSIS limitations, it was considered one vertical fault plane with L= 80 km and W= 16 km, divided into 15×9=135 subfaults.

The fault rupture displacement pattern adopted (Figure 6) was adjusted from a study made for the fault rupture (Peyrat *et al.*, 2001). For each simulation and subfault, it was introduced a random variation of 1±0.25.

It was adopted a static stress drop of 110 bars (Fletcher and McGarr, 2006), with β=3.7 km/s, ρ=2.8 g/cm^3, V_r=2.7 km/s, and ΔL_r=20 km.

The path attenuation expressions adopted results from studies made for North America (Atkinson and Boore, 1995).

No soil effects were considered, k_0= 0 and with cut-off frequency f_{max} equal to 8 Hz (Pearblossom/Pallet Creek), 12 Hz (Silent Valley/Poppet Flat) and 14 Hz (Lake Cahuilla/County Park).

The effective duration prediction was obtained with an empirical expression deduced from more then 800 Mexican records (Reinoso and Ordaz, 2001), which consider the three components of duration.

Figure 5 – Fault rupture localization

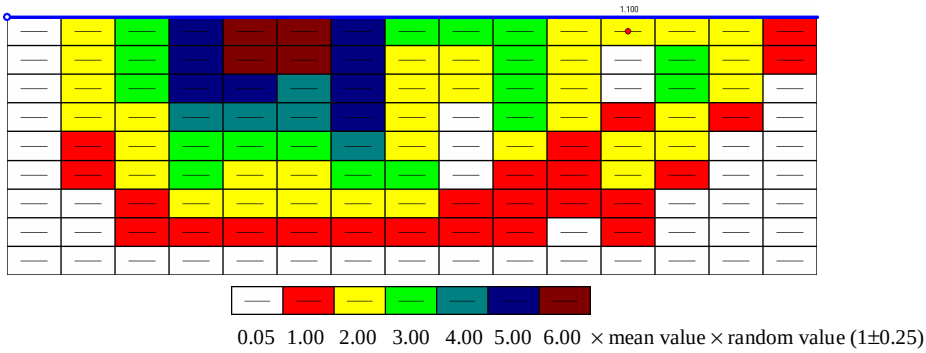

Figure 6 – Fault rupture displacement pattern considered for the simulations of 1992's Landers earthquake

Simulations where made with variable radiation pattern and expression (11), as described earlier. The response spectra are presented in Figures 7 to 9.

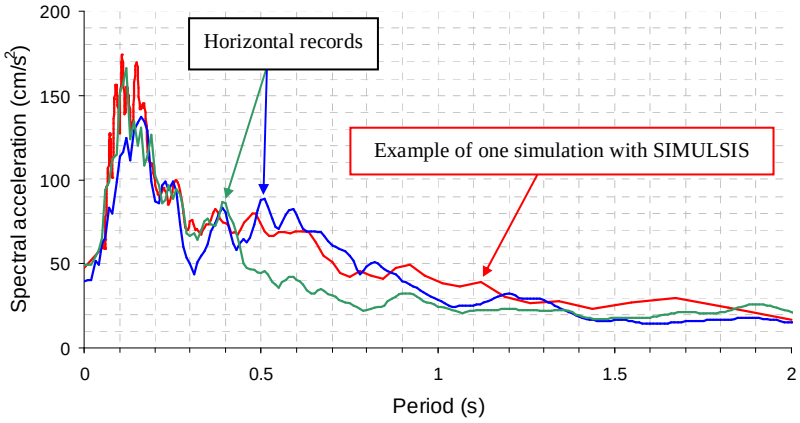

Figure 7 – Response spectra comparison at Silent Valley/Poppet Flat (56 km)

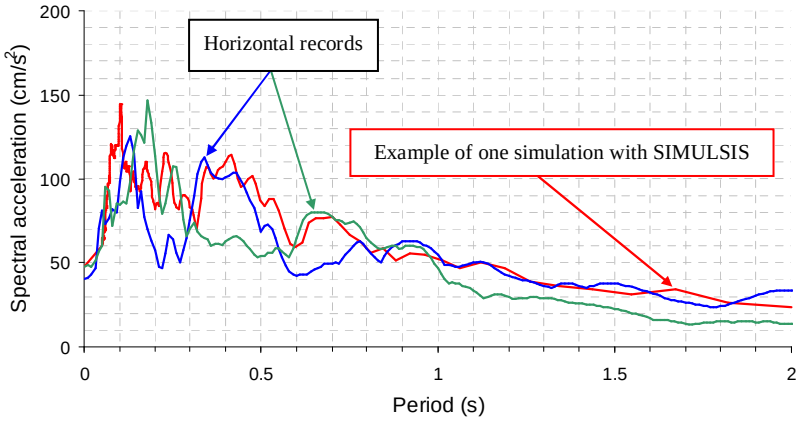

Figure 8 – Response spectra comparison at Lake Cahuilla/County Park (67 km)

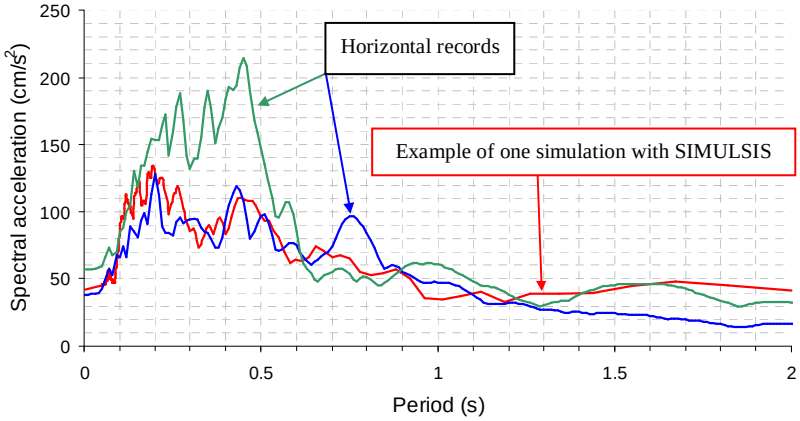

Figure 9 – Response spectra comparison at Pearblossom/Pallet Creek (138 km)

4. SIMULATION OF THE 1 JANUARY 1980 AZORES EARTHQUAKE

The 1980's Azores earthquake affected a large percentage of the building stock in the islands of S. Jorge, Graciosa and Terceira with evidence of directivity and local site effects (Malheiro, 2006; Oliveira, 1992; Teves-

Costa *et al.*, 2007). Epicentre coordinates where 38.81ºN, 27.78ºW with depth focus about 10 km, and the assigned moment magnitude is M_w= 6.9 (NEIC).

In these simulations we considered a plane fault with L= 30 km and W= 10 km, divided into 15×5=75 subfaults (Figure 10), with two asperities representing 22% of total fault area (Somerville *et al.*, 1999).

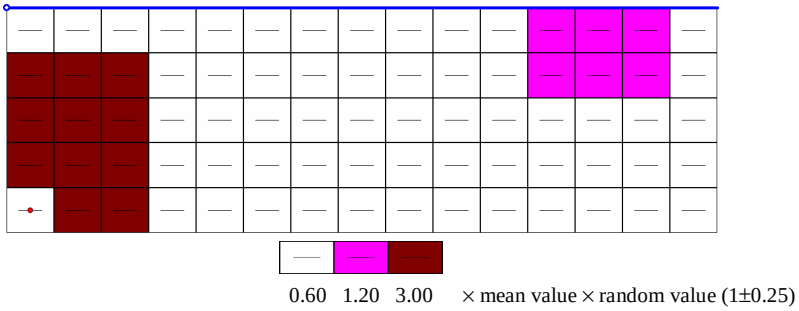

Figure 10 – Fault rupture displacement pattern considered for the simulations of 1980's Azores earthquake

The strike (149º) and dip (85º) considered were the proposed in other studies (Borges *et al.*, 2007a), as well the rupture velocity of 1.8 km/s. The seismic moment was obtained from an empirical equation (Hanks and Kanamori, 1979).

The simulations were made with constant radiation pattern (=0.55) and with expression (11), for several places (considering k_0=0), where strong motion records exist (Horta), and also where exists an estimation of peek ground motion based on studies related to the seismic response of several structures (Oliveira *et al.*, 1992):

• "Observatório Príncipe do Mónaco" in Horta, Faial – simulations considering soil effects (35 m of soil layers with increasing shear wave velocity, with a mean value of 165 m/s) and f_{max}= 7 Hz.

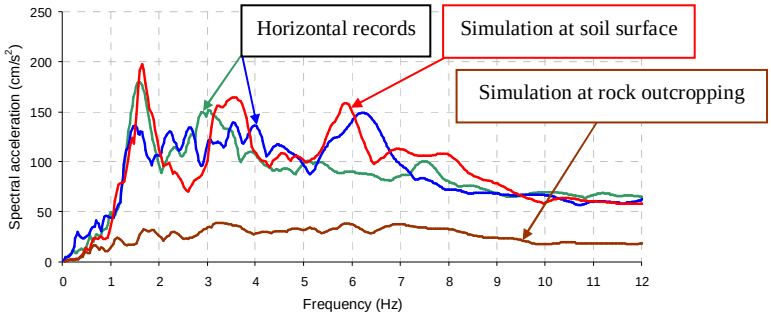

Figure 11 – Response spectra comparison at "Observatório Príncipe do Mónaco" in Horta (80 km)

• "Semáforo do Monte Brasil" in Angra do Heroísmo, Terceira – simulations at rock outcropping with f_{max}= 15 Hz, which were compared with type 1 (soil I) response spectra of Portuguese code (RSAEEP, 1983) adjusted to the peek value of 27 cm/s^2 as proposed by Oliveira *et al.* (1992) as a result of observed structural behaviour.

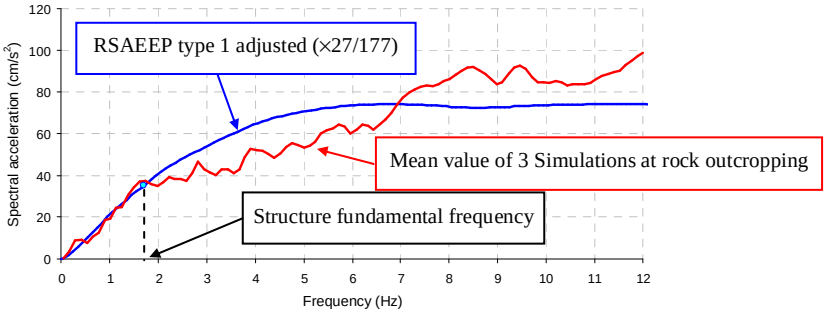

Figure 12 – Response spectra comparison at "Semáforo do Monte Brasil" in Angra do Heroísmo (52 km)

• Hospital of Angra do Heroísmo, Terceira – simulations considering soil effects (20 m of soil layers with increasing shear wave velocity, with a mean value of 160 m/s) and f_{max}= 15 Hz, which were compared with the type 2 (soil III) response spectra of Portuguese code (RSAEEP, 1983) adjusted to the peek value of 144 cm/s^2 as proposed by Oliveira *et al.* (1992) based on the observed structural behaviour (first 13 modes between 1.36 and 6.1 Hz).

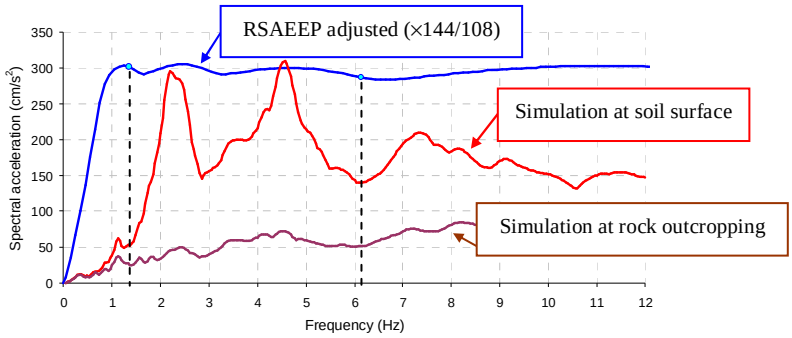

Figure 13 – Response spectra comparison at Hospital of Angra do Heroísmo (52 km)

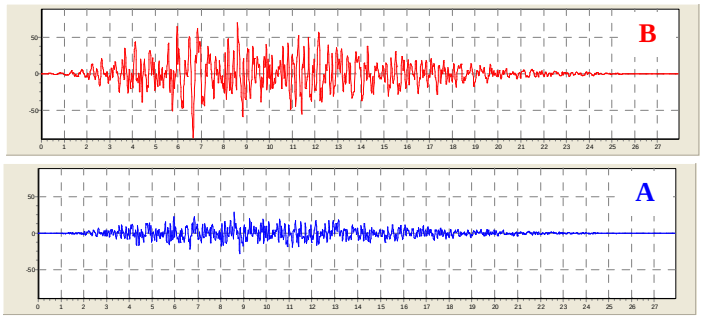

Figure 14 – Simulated accelerograms at Angra's Hospital for (A) rock outcropping and (B) soil surface

• "Semáforo da Praia da Vitória", Terceira – simulations made with the same parameters of those made for Monte Brasil.

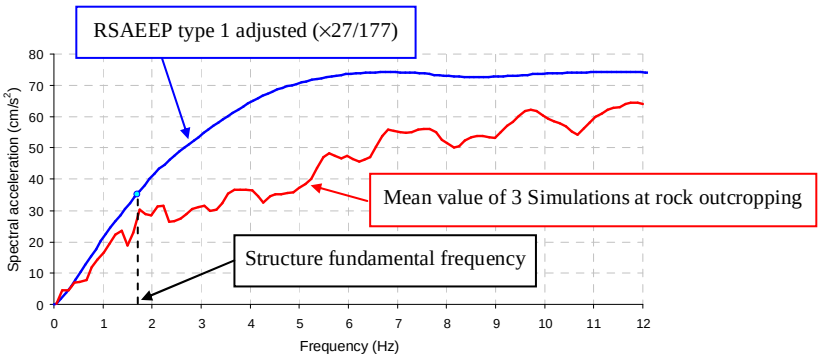

Figure 15 – Response spectra comparison at "Semáforo da Praia da Vitória" in Terceira (63 km)

• Lighthouse of Topo, S. Jorge – simulations made with the same soil column as for the "Observatório Príncipe do Mónaco" in Horta, Faial, but with f_{max}= 15 Hz. The fundamental frequency of the lighthouse is around 3 Hz and a spectral acceleration of 1.3g was proposed by Oliveira *et al.* (1992).

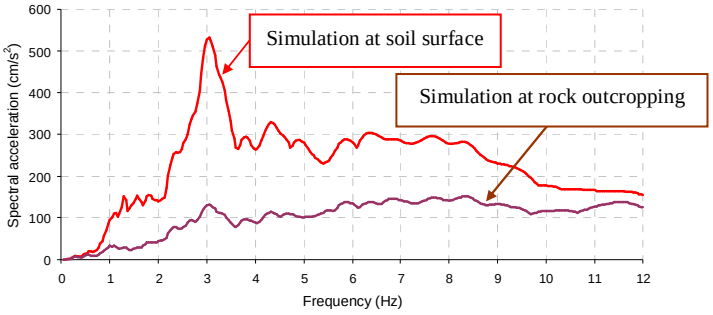

Figure 16 – Response spectra comparison at Lighthouse of Topo in S. Jorge (30 km)

5. CONCLUSIONS

From the comparison between the simulations and records obtained for the Landers earthquake, it seems that the program SIMULSIS is a powerful tool with the ability to reproduce a good approximation of earthquake motions, for structural analysis purposes.

The program was able to reproduce the peek ground acceleration of 1992 Landers earthquake and reproduce a good approximation of Silent Valley/Poppet Flat and Lake Cahuilla/County Park recorded response spectra. For the Pearblossom/Pallet Creek site the program managed to reproduce a good approximation of one record component, but not the other. That could be related to the differences between the real source rupture and the fault plane adopted for the simulations. Other possibility is simply the incapacity of the algorithm to completely reproduce the directivity effects.

The simulations of 1980 Azores earthquake, namely at "Observatório Príncipe do Mónaco" in Horta, Faial, and at Hospital of Angra do Heroísmo, Terceira, show the importance of local soil effects in peek acceleration and in spectral acceleration, most important for structural response. Simulations response spectra are well related to damage observed at those places, except for the lighthouse of Topo in S. Jorge, where the maximum spectral acceleration obtained was lower than expected. That could be related to a similar problem verified for the simulations of 1992's Landers earthquake at Pearblossom/Pallet Creek site, so further studies must be made.

Computer tools like this are very important for damage assessment, because they allow the study of the individual contribution of earthquake characteristics to structural response.

In further developments the possibility of multiple faults planes and non constant rupture velocity will be considered.

6. REFERENCES

Atkinson, G. M., and D. M. Boore (1995) Ground-Motion Relations for Eastern North America. *Bulletin of the Seismological Society of America* 85(1), 17-30.

Bommer, J. J., and A. Martinez-Pereira (1999) The effective duration of earthquake strong motion. *Journal of Earthquake Engineering* 3(2), 127-172.

Bommer, J. J., and A. B. Acevedo (2004) The use of real earthquake accelerograms as input to dynamic analysis. *Journal of Earthquake Engineering* 8(Special Issue 1), 43-92.

Boore, D. M. (1983) Stochastic simulation of high-frequency ground motions based on seismological models of the radiated spectra. *Bulletin of the Seismological Society of America* 73(6), 1865-1894.

Boore, D. M., and J. Boatwright (1984) Average body-wave radiation coefficients. *Bulletin of the Seismological Society of America* 74(5), 1615-1621.

Boore, D. M. (2003) Simulation of Ground Motion Using the Stochastic Method. *Pure and Applied Geophysics* 160, 635-676.

Boore, D. M. (2005) SMSIM — Fortran programs for simulating ground motions from earthquakes:Version 2.3 - A Revision of OFR 96–80–A, 55 pp, U.S. Geological Survey, Menlo Park.

Borges, J. F., M. Bezzeghoud, E. Buforn, C. Pro, and A. Fitas (2007a) The 1980, 1997 and 1998 Azores earthquakes and some seismo-tectonic implications. *Tectonophysics* 435(1-4), 37-54.

Borges, J. F., B. Caldeira, R. Grandin, M. Bezzeghoud, and F. Carrilho (2007b) Modelação pelo método das diferenças finitas dos movimentos sísmicos em Portugal Continental - Algumas implicações para o sismo de 1755. 7º Congresso de sismologia e engenharia sísmica, FEUP, Porto. (in portuguese)

Campos Costa, A., M. L. Sousa, A. Carvalho, J. Bilé Serra, A. Martins, and E. Cansado Carvalho (2004) Simulador de cenários sísmicos integrados num sistema de informação geográfica. 6º Congresso Nacional de Sismologia e Engenharia Sísmica, Universidade do Minho, Guimarães. (in portuguese)

Campos Costa, A., M. L. Sousa, A. Carvalho, and E. Coelho (2006) Seismic loss scenarios based on hazard disaggregation. Aplication to the metropolitan region of Lisbon, Portugal. In *Assessing and managing earthquake risk*. edited by C. S. Oliveira, A. Roca and X. Goula, pp. 449-462, Springer, Dorrecht.

CEN (2004) *Eurocode 8, Design of Structures for Earthquake Resistance-Part 1: general rules, seismic actions and rules for buildings. EN 1998-1: 2004*, 229 pp., Comité Européen de Normalisation.

CodeGear (2007) Delphi 2007 for Win32, Professional Edition, Borland.

Erdic, M., and E. Durukal (2006) Strong ground motion. In *Recent advances in Earthquake Geotechnical Engineering am Microzonation.* edited by A. Ansal, pp. 67-100, Springer, Dorrecht.

Fletcher, J. B., and A. McGarr (2006) Distribution of stress drop, stiffness, and fracture energy over earthquake rupture zones. *Journal of Geophysical Research* 111(B03312), 1-12.

Furumura, T. (2005) Large-scale parallel simulation of seismic wave propagation and strong ground motions for the past and future earthquakes in Japan. *Journal of the Earth Simulator* 3, 1-10.

Gupta, I. D., and M. D. Trifunac (1996) Investigation of nonstationarity in stochastic seismic response of structures, 180 pp, University of Southern California, Department of Civil Engineering, Los Angeles.

Hanks, T. C., and H. Kanamori (1979) A moment magnitude scale. *Journal of Geophysical Research* 84(B5), 2348-2350.

Idriss, I. M., and J. I. Sun (1992) User's manual for SHAKE91: a computer program for conducting equivalent linear seismic response analyses of horizontally layered soil deposits, 13 pp, University of California, Davis.

Kramer, S. L. (1996) *Geotechnical earthquake engineering*, 653 pp., Prentice Hall, Inc, New Jersey.

Lee, V. W. (1995) Generation of synthetic time histories of ground motion. In *Selected topics in Probabilistic Seismic Hazard Analysis - Report No. CE 95-08*. edited by M. I. Todorovska, I. D. Gupta, V. K. Gupta, V. W. Lee and M. D. Trifunac, pp. VI.1-VI.54, University of Southern California, Los Angeles.

Lee, V. W. (2002) Empirical scaling of strong earthquake ground motion-part II: duration of strong motion. *ISET Journal of Earthquake Technology* 39(4, Paper No. 426), 255-271.

Malheiro, A. (2006) Geological hazards in the Azores archipelago: Volcanic terrain instability and human vulnerability. *Journal of Volcanology and Geothermal Research* 156(1-2), 158-171.

Motazedian, D., and G. M. Atkinson (2005) Stochastic finite-fault modeling based on a dynamic corner frequency. *Bulletin of the Seismological Society of America* 95(3), 995-1010.

Motazedian, D., and A. Moinfar (2006) Hybrid stochastic finite fault modeling of 2003, M6.5, Bam earthquake (Iran). *Journal of Seismology* 10(1), 91-103.

Oliveira, C. S. (1992) Quantificação do movimento sísmico aquando do sismo de 1 de Janeiro de 1980. In *10 anos após o sismo dos Açores de 1 de Janeiro de 1980, volume 1*. edited by C. S. Oliveira, A. R. A. Lucas and J. H. C. Guedes, pp. 83-125, Governo Regional dos Açores and LNEC, Lisboa. (in portuguese)

Oliveira, C. S., M. R. Corrêa, and A. Martins (1992) Comportamento dinâmico de algumas estruturas de betão armado durante o sismo. In *10 anos após o sismo dos Açores de 1 de Janeiro de 1980, volume 2*. edited by C. S. Oliveira, A. R. A. Lucas and J. H. C. Guedes, pp. 481-518, Governo Regional dos Açores and LNEC, Lisboa. (in portuguese)

Peyrat, S., K. Olsen, and R. Madariaga (2001) Dynamic modeling of the 1992 Landers earthquake. *Journal of Geophysical Research* 106(B11), 26,467–426,482.

Reinoso, E., and M. Ordaz (2001) Duration of strong ground motion during Mexican earthquakes in terms of magnitude, distance to the rupture area and dominant site period. *Earthquake Engineering & Structural Dynamics* 30(5), 653-673.

RSAEEP (1983) *Regulamento de Segurança e Acções em Estruturas de Edifícios e Pontes*, Dec-Lei nº 235/83 de 31 de Maio. (in portuguese)

Schnabel, P. B., J. Lysmer, and H. B. Seed (1972) SHAKE: A computer program for earthquake response analysis of horizontally layered sites, Report EERC 72-12, 92 pp, Earthquake Engineering Research Center, University of California, Berkeley.

Sieh, K., L. Jones, E. Hauksson, K. Hudnut, D. Eberhart-Phillips, T. Heaton, S. Hough, K. Hutton, H. Kanamori, A. Lilje, S. Lindvall, S. F. McGill, J. Mori, C. Rubin, J. A. Spotila, J. Stock, H. K. Thio, J. Treiman, B. Wernicke, and J. Zachariasen (1993) Near-Field Investigations of the Landers Earthquake Sequence, April to July 1992. *Science* 260(5105), 171-176.

Somerville, P., K. Irikura, R. Graves, S. Sawada, D. Wald, N. Abrahamson, Y. Iwasaki, T. Kagawa, N. Smith, and A. Kowada (1999) Characterizing earthquake slip models for the prediction of strong ground motion. *Seismological Research Letters* 70(1), 59-80.

Stewart, J. P., S.-J. Chiou, J. D. Bray, R. W. Graves, P. G. Somerville, and N. A. Abrahamson (2001) Ground motion evaluation procedures for performance-based design, 229 pp, Pacific Earthquake Engineering Research Center, Berkeley.

Teves-Costa, P., C. S. Oliveira, and M. L. Senos (2007) Effects of local site and building parameters on damage distribution in Angra do Heroísmo—Azores. *Soil Dynamics and Earthquake Engineering* 27(11), 986-999.

Udías, A. (1999) *Principles of seismology*, 475 pp., Cambridge University Press, Cambridge.